Bioactive properties and gut microbiota modulation by date seed polysaccharides extracted using ultrasound-assisted deep eutectic solvent

Athira Jayasree Subhash [a], Gafar Babatunde Bamigbade [a], Mohammed Tarique [a], Basel Al-Ramadi [b], Basim Abu-Jdayil [c], Afaf Kamal-Eldin [a], Laura Nyström [d], Mutamed Ayyash [a,e,*]

[a] *Department of Food Science, College of Agriculture and Veterinary Medicine, United Arab Emirates University (UAEU), Al-Ain, United Arab Emirates*
[b] *Department of Medical Microbiology and Immunology, College of Medicine and Health Sciences, United Arab Emirates University (UAEU), Al Ain, United Arab Emirates*
[c] *Chemical and Petroleum Engineering Department, College of Engineering, United Arab Emirates University (UAEU), PO Box 15551, Al Ain, United Arab Emirates*
[d] *Department of Health Science and Technology, Institute of Food, Nutrition and Health, ETH Zurich, 8092 Zurich, Switzerland*
[e] *Zayed Center for Health Sciences, United Arab Emirates University (UAEU), Al Ain, United Arab Emirates*

ARTICLE INFO

ABSTRACT

Polysaccharides are abundant macromolecules. The study extracted date seed polysaccharides (UPS) using ultrasound-assisted deep eutectic solvent extraction to valorize date seeds. UPS were subjected to comprehensive characterization and evaluation of their bioactivity, prebiotic properties, and their potential to modulate the gut microbiome. Characterization revealed UPS's heteropolysaccharide composition with galactose, mannose, fructose, glucose, and galacturonic acid respectively in 66.1, 13.3, 9.9, 5.4, and 5.1%. UPS showed a concentration-dependent increase of radical scavenging and antioxidant activities, evidenced by FRAP, TAC, and RP assays. They also displayed antimicrobial efficacy against *E. coli* O157:H7, *S. typhimurium*, *S. aureus*, and *L. monocytogenes*. Rheological analysis showed UPS's elastic-dominant nature with thixotropic tendencies. UPS inhibited α-glycosidase, α-amylase, and ACE up to 86%, and reduced Caco-2 and MCF-7 cell viability by 70% and 46%, respectively. UPS favored beneficial gut microbiota growth, releasing significant SCFAs during fecal fermentation.

1. Introduction

According to Food and Agriculture Organization Statistics (FAO-STAT, 2023), date production has escalated globally over the past decade, rising from 7.53 to 9.6 million metric tonnes. Reports indicate that date seed waste contributes approximately 852 thousand tonnes annually to post-harvest loss (Bouaziz, Ben Abdeddayem, Koubaa, Ellouz Ghorbel, & Ellouz Chaabouni, 2020). Date product processing industries, producing items like paste and syrup, significantly add to this waste. The *Phoenix dactylifera* yields an edible fleshy pericarp and a seed—often discarded or used in animal feed—that constitutes 10–15% of the fruit's weight (Ghnimi, Umer, Karim, & Kamal-Eldin, 2017). These seeds, containing fibers (64–80 g/100 g) (mainly insoluble fiber-hemicellulose, cellulose, lignin), tannins (31.3 mg/g catechin

equivalents), proteins (5.1 g/100 g), and polyphenols (11.8 mg GAE/g seed), offer antioxidant and antimicrobial benefits (Barakat, Hamed, Bassuiny, Abdel-Aty, & Mohamed, 2020; El Sheikh, El-Kholany, & Kamel, 2014). They are linked to health benefits such as mitigating hypertension and heart disease and supporting gut microbiota (Al-Farsi & Lee, 2011; Al-Thubiani & Ahmad Khan, 2017). Predominant polysaccharides like arabinoxylans and galactomannan enhance their value in functional food applications due to the effective release of dietary fiber in the human body (Ishrud, Zahid, Zhou, & Pan, 2001; Noorbakhsh & Khorasgani, 2023). Yet, despite their nutritional components, date pits are typically underused.

Polysaccharides (PS), abundant natural polymers, vary in monosaccharide composition, chain length, and branching, molecular weight distribution patterns *etc.* (Mohammed, Naveed, & Jost, 2021). Their role in food matrices is notable, given their antioxidant, antimicrobial, and health-promoting qualities (Gao et al., 2020; Zhou et al., 2022). Date seeds are primarily composed of these bioactive polysaccharides, with β-1,4-linked D-xylose, arabinose, galactose, and acetyl groups forming the central hemicellulose structure (Noorbakhsh & Khorasgani, 2023).

Traditional methods for extracting polysaccharides (PS) often fall short in terms of efficiency, due to low yields and limited opportunities for reusing materials. Additionally, these methods can introduce harmful substances into the environment. To address these issues, researchers are turning to alternative techniques that don't rely on heat, such as using sound waves (ultrasound), microwaves, and electrical pulses (pulsed electric field) alongside environmentally friendly solvents (Huang et al., 2017; Zhou et al., 2022). One promising option is Deep Eutectic Solvents (DESs), which are safe, stable, and can be reused, making them a more sustainable choice for obtaining plant-based bioactive compounds (Huang et al., 2017). When used in combination with ultrasonic waves, DESs have proven to be a powerful and green method for extracting valuable polysaccharides from plant leftovers (Huang et al., 2017; Li, Li, Luo, Ma, & Liu, 2019). After extraction, it's important to study how these polysaccharides change during digestion and fermentation because this influences their ability to support good gut health, especially their function as prebiotics that nourish beneficial gut bacteria (Han et al., 2022). Polysaccharides typically resist digestion until reaching the colon, where they support beneficial bacteria and contribute to SCFA production (Han et al., 2022). Their fermentation can improve bowel health, aiding in disease prevention and toxin elimination (Ho Do, Seo, & Park, 2021).

Previous studies have extracted polysaccharides from date seeds, but the use of novel non-thermal green techniques like Ultrasound-assisted Deep Eutectic Solvent extraction has not been explored. Additionally, the behavior of these polysaccharides during digestion and their effect on the gut microbiome remains under-researched. This study aimed to: i) extract, purify, and characterize date seed polysaccharides (UPS) using ultrasound and DESs, analyzing their physicochemical, bioactive, antioxidant, and rheological properties; ii) assess the digestion and fermentation of polysaccharides, their prebiotic impact on probiotics, and their influence on the gut microbiome through *in vitro* fecal fermentation.

2. Materials and methods

2.1. Extraction of polysaccharides from date seeds

2.1.1. Raw material preparation

Date seeds were milled into a fine powder using a Retsch ZM200 DR100 miller (Haan, Germany) and then defatted through a double hexane extraction method, following the procedure outlined by Yang, Zamani, Liang, and Chen (2021). The defatted date seeds were preserved for subsequent extraction and analysis.

2.1.2. Ultrasound-assisted deep eutectic solvent extraction of DSPs

A deep eutectic solvent (DES), composed of choline chloride as the

hydrogen bond acceptor (HBA) and ethylene glycol as the hydrogen bond donor (HBD), was synthesized with slight modifications to the method described by Gao et al. (2020). The HBA and HBD were mixed in a 1:1 M ratio using a magnetic-assisted hotplate (Stuart, United Kingdom) at 100 °C until a clear and homogeneous solution was achieved. A fraction of water (10% *v/v*) was added to adjust the viscosity of the DES. The effectiveness of each DES was assessed in terms of viscosity and the yield of extracted polysaccharides.

Before the ultrasound processing, the operating conditions for DES extraction were further optimized to study the interaction between factors and maximize DSP extraction efficiency. A three-level Central Composite design (CCD) with four factors was employed using Design-Expert 8.0 to optimize the extraction conditions. The independent variables, including pH (2, 5, 8), extraction time (30, 75, 120 min), extraction temperature (50, 75, 100 °C), and solid–liquid ratio (10, 35, 60 mg/mL), were tested for their impact on concentration of the extracted DSP. The experimental data from the CCD were subsequently modeled and optimized using response surface methodology (RSM) with a second-order polynomial model. Date seed extraction was performed while keeping the optimized DES conditions constant but varying ultrasound parameters using a Branson 550 probe-type ultrasound (Mexico) (Li et al., 2019). A three-level CCD with two independent factors, time (5, 12.5, 20 min) and amplitude (40, 60, 80 Hz), was assessed against extracted polysaccharide concentration (mg/mL). From this point forward, the extracted polysaccharide from the date seed was referred to as UPS.

2.1.3. Purification of UPS

About 50 g of defatted date seeds underwent ultrasound-assisted DES extraction as outlined in section 2.1.2. The resulting mixture was centrifuged at 4 °C, and the residue was discarded. The supernatant was then mixed with 16% trichloroacetic acid (TCA) to achieve an 8% TCA solution and stored at 4 °C for 1 h. Following this, two volumes of absolute chilled ethanol were added to the supernatant and left at 4 °C for 24 h. Centrifugation was conducted at 15000 ×g, 4 °C for 20 min, and the resulting precipitate was dissolved in warm deionized water. Subsequently, the mixture was transferred into a 20 kDa MWCO Slide-A-Lyzer G2 dialysis cassette (Thermo Fisher Scientific, USA) and dialyzed against deionized water for 72 h at 4 °C. The yield of the extracted polysaccharide (UPS) was determined using the phenol-sulfuric acid method (DuBois, Gilles, Hamilton, Rebers, & Smith, 1956). A portion of the partially-purified UPS was allocated for bioactivity assessment, while the remainder was freeze-dried and stored at −20 °C for further analysis.

2.2. UPS characterization

2.2.1. Determination of average molecular weight and monosaccharide composition

The molecular weight (Mw) of the UPS was assessed using gel permeation chromatography (GPC), following the procedure described by Al-Nabulsi et al. (2022). In brief, the freeze-dried crude UPS was filtered through 0.22 μm syringe filters and subsequently injected into the SIL-20 AC autosampler of the Shimadzu HPLC system (Japan), equipped with a refractive index detector (RID-20 A) using distilled water as mobile phase. For detection, a Shim-pack GPC-802 column maintained at 40 °C was utilized, and the elution was carried out with deionized water as mobile phase at a flow rate of 1 mL/min. Mw was determined based on a calibration curve established using various pullulan standards (Mw = 800, 400, 200, 110, 50, 22, 10, 6, 1.3, and 0.342 kDa).

The monosaccharide composition of UPS was determined with slight modifications to a two-step acid hydrolysis method, as outlined by Shi et al. (2020). The purified UPS underwent concurrent treatment with 2 M trifluoroacetic acid (TFA) and 72% H_2SO_4. Subsequently, the supernatant was subjected to 1-phenyl-3-methyl-5-pyrazolone (PMP)

derivatization (Vojvodić Cebin, Komes, & Ralet, 2022). The filtered and derivatized UPS sample was analyzed on a Thermo C18 column (250 × 4.6 mm, 5 μm) within a Shimadzu HPLC system equipped with an SPD-M20A photodiode array detector (PDA-245 nm). A gradient program was developed with varying mobile phase compositions (A: 0.1 M Phosphate buffer, B: Acetonitrile), a flow rate of 1.5 mL/min, and a column temperature of 30 °C.

2.2.2. FT-IR spectroscopy (FT-IR)

The purified and freeze-dried UPS underwent FT-IR analysis following the procedure described by Ayyash et al. (2020). The UPS was positioned on a Diamond/ZnSe crystal plate (Perkin-Elmer Inc.), and 16 scans were conducted, each with a scanning resolution of ± 4 cm^{-1}, over the range of 400 to 4000 cm^{-1}.

2.2.3. Differential scanning calorimetry (DSC) and Thermo-gravimetric analysis (TGA)

DSC was employed to determine the melting point of UPS. Approximately 5–10 mg of the sample was analyzed using a DSC 25 instrument (TA Instruments, New Castle, DE, USA), in accordance with Al-Hamayda, Abu-Jdayil, and Ayyash (2023). Additionally, Thermo Gravimetric Analysis of the purified, freeze-dried UPS was conducted on a TGA instrument (TGA-2 star system, Mettler Toledo) to assess the thermal weight loss stages of the UPS (Tan et al., 2020).

2.2.4. Zeta potential and particle size analysis

The purified and freeze-dried UPS was subjected to particle size and zeta potential analysis using a NanoPlus Zeta Potential & Particle Size Analyzer from Particulate Systems (GA, USA), in accordance with the procedure outlined by Ayyash et al. (2020).

2.2.5. SEM analysis

The surface morphology of the freeze-dried UPS was determined using an Analytical Scanning Electron Microscope (JEOL JSM-6010/ LA, Tokyo, Japan) equipped with a secondary electron imaging mode (Ayyash, Al-Nuaimi, Al-Mahadin, & Liu, 2018). SEM measurements were conducted at 20 kV by coating gold coating the UPS using a Cressington 108 Auto Sputter Coater (Ted Pella Inc., Redding, CA, USA) and images were recorded within the magnification range of 50-3000×.

2.2.6. Functional properties of UPS

The functional properties of UPS, namely the Water Solubility Index (WSI), Water Holding Capacity (WHC), and Oil Holding Capacity (OHC), were determined according to Jiang et al. (2021) and calculated using the following equations:

$$\text{WSI\%} = \frac{\text{Dry solid weight}}{\text{Total solid weight}} \times 100 \quad (1)$$

$$\text{WHC\%} = \frac{\text{Water bound weight}}{\text{Total solid weight}} \times 100 \quad (2)$$

$$\text{OHC\%} = \frac{\text{Oil bound weight}}{\text{Total solid weight}} \times 100 \quad (3)$$

2.2.7. Rheological properties of UPS

The rheological properties of UPS were assessed using a cone plate, Peltier plate Steel (760 mm) on a Rheometer (Discovery Hybrid HR-2, TA Instruments, DE, USA), with modifications to the method of Ayyash et al. (2020). The linear viscoelastic region of the samples was determined through an amplitude sweep method at a constant frequency of 1.0 Hz, varying the strain between 0.1 and 10%. A frequency sweep test was conducted to evaluate the viscoelastic behavior of the samples, with the frequency ranging from 0.1 to 50 Hz at a constant strain of 0.5% within the linear viscoelastic region. The thixotropic behavior of the UPS sample was measured using the time sweep method, and the storage (G′)

and loss (G″) moduli were recorded at a frequency of 1.0 Hz. Three-time segments were applied: 1) first (200 s, stress 0.8 Pa), 2) second (100 s, stress 50 Pa), and third (400 s, stress 0.8 Pa). Data were analyzed using TRIOS 5.2 software.

2.3. Evaluation of biological activities of UPS

The details of the biological activities of UPS at different concentrations (125, 250, 500, 1000 μg/mL) were detailed in (Subhash et al., 2024) unless otherwise mentioned. A brief of each trait was as follows:

2.3.1. Determination of antioxidant potential

2.3.1.1. DPPH and ABTS radical scavenging activities.
The scavenging activity of the purified UPS against 1,1-diphenyl-2-picrylhydrazyl (DPPH) and 2,2′-azino-bis(3-ethylbenzene-thiazoline-6-sulphonic acid) radical (ABTS•+) was evaluated at 517 nm and 734 nm, respectively (Gulcin & Alwasel, 2023). The scavenging rate was calculated using eq. 4:

$$\text{Scavenging rate (\%)} = \frac{(\text{Blank}_{\text{Abs}} - \text{UPS}_{\text{Abs}})}{\text{Blank}_{\text{Abs}}} \times 100 \quad (4)$$

2.3.1.2. Superoxide scavenging activities.
The superoxide scavenging activity of UPS, in terms of superoxide dismutase (SD) and superoxide anion scavenging (SAS) activity, was measured at 420 nm and 320 nm, respectively. The rate of pyrogallol oxidation inhibition was calculated using Eq. 4.

2.3.1.3. Reactive oxygen scavenging activities.
The inhibition of reactive oxygen by UPS, in terms of hydrogen peroxide and hydroxyl radical scavenging activity at 230 nm and 536 nm, respectively, was determined. The scavenging activity was calculated using Eq. 4.

2.3.1.4. Metal chelation.
The ability of purified UPS to prevent oxidative stress was determined through metal chelating activity and inhibition of lipid peroxidation at 562 nm and 532 nm, respectively (Gulcin & Alwasel, 2022). The inhibition of oxidative stress was calculated using the scavenging rate Eq. 4.

2.3.1.5. FRAP, reducing power (RP) and Total antioxidant capacity (TAC).
The antioxidant power of purified UPS was determined through ferric reducing antioxidant power (FRAP) and reducing power (RP) assays, and Total Antioxidant Capacity (TAC) was measured (Mutlu et al., 2023). The standard curve of ascorbic acid (100–1000 μg/mL) were plotted at 593 nm, 700 nm, and 695 nm for FRAP, RP, and TAC, respectively. The results were calculated in terms of μg/mL equivalent to ascorbic acid.

2.3.2. Minimum inhibitory concentrations

Inhibition studies of UPS at different concentrations (mg/mL) against common foodborne pathogens, including *Escherichia coli* 0157: H7 1934, *Salmonella Typhimurium* 02–8423, *Staphylococcus aureus* ATCC 25923, and *Listeria monocytogenes* DSM 20649, were conducted following the method by Tarique et al. (2022).

2.3.3. Antiproliferative properties

The anticancer properties of UPS on the Caco-2 and MCF-7 cancer cell lines were evaluated as per the method described by Ayyash et al. (2018). The antiproliferative was calculated using the following formula:

$$\text{Antiproliferative (\%)} = \left[1 - \frac{R_{sample} - R_o}{R_{contorl} - R_o} \right] \times 100 \quad (5)$$

where R_{sample} is the absorbance ratio of OD570/OD605 in the

presence of UPS. R$_{control}$ is the absorbance ratio of OD570/OD605 in the absence of UPS [vehicle (positive) control]. R$_O$ is the averaged background [non-cell (negative) control] absorbance ratio of OD570/OD605.

2.3.4. α-amylase and α-glycosidase inhibition activities

The inhibition of α-amylase and α-glycosidase was used to assess the antidiabetic activity of UPS (Ayyash et al., 2018). The absorbance was recorded at 540 and 400 nm for α-amylase and α-glycosidase, respectively. The rate of inhibition was calculated using the following equation:

$$\text{Inhibition } (\%) = \frac{(\text{Blank}_{Abs} - \text{UPS}_{Abs})}{\text{Blank}_{Abs}} \times 100 \tag{6}$$

2.3.5. Angiotensin-converting enzyme (ACE) inhibition

UPS was evaluated for ACE inhibitory activity according to Ayyash et al. (2018) at 228 nm. The inhibition was calculated using Eq. 6.

2.4. Total and reducing sugar contents after in vitro digestion

In vitro digestion of the purified UPS was performed following the method by Ayyash et al. (2021). The digesta was stored at −20 °C for further investigation of the reducing sugar and total sugar content before and after digestion (DuBois et al., 1956; Han et al., 2022).

2.5. Prebiotic properties of UPS

The prebiotic effects of UPS on 6 probiotic strains, including *Lactobacillus acidophilus* DSMZ 9126, *Lactobacillus delbrueckii* subsp. *delbrueckii* DSMZ 20074, *Lacticaseibacillus rhamnosus* DSMZ 20021, *Lacticaseibacillus paracasei* subsp. *paracasei* DSMZ 20207 and *Lactobacillus gasseri* DSMZ 20243 were determined according to Yılmaz and Şimşek (2020). The growth kinetics of each probiotic strain with different carbon sources were measured at 600 nm for 24 h at 15-min intervals.

2.6. In vitro fecal fermentation

2.6.1. In vitro fecal fermentation

The fecal slurry was prepared from fresh fecal samples collected from healthy individuals aged 24–40 who had not recently been administered antibiotics. Fecal fermentation was performed by mixing the fecal slurry with basal medium, following a modification of the method by Han et al. (2022). Then, 2.5 mL of the supernatant was mixed with 5 mL of sterilized fermentation medium with 2% UPS and 2% of GOS-P (control group), respectively, and the fermentation medium without additional carbon source (blank group) was set as the negative control group under the same conditions, followed by incubating them at 37 °C in a shaking water bath for 24 h.

2.6.2. Monitoring fecal fermentation

The changes in pH, total sugar, gas production, and reducing sugar during fecal fermentation of UPS were examined according to Han et al. (2022) at 0, 6, 12, 24, and 48 h.

2.6.3. Quantitative evaluation of short-chain fatty acid production

SCFAs produced after the fecal fermentation of UPS were determined according to Dobrowolska-Iwanek et al. (2020) with minor modifications. After 48 h of fecal fermentation, the broth was centrifuged at 15,000 ×*g* for 20 min, and the supernatant was filtered using 0.45 μm filters. HPLC system equipped with an SPD-M20A photodiode array detector (PDA) (Shimadzu, Japan), and Shodex C18M 4E (250 × 4.6 mm, 5 μm) column (Resonac Inc., Japan) was used with an isocratic mobile phase containing 10 mM Monopotassium Phosphate (pH 2.4) with phosphoric acid and 100% acetonitrile (80:20) at a flow rate of 1.5

mL/min at a column temperature of 30 °C. The injection volume was set to 20 μL for a runtime of 7 min with the UV detector set at 210 nm. Standard calibration curves were prepared for acetic acid, propionic acid, and butyric acid under similar conditions (62.5, 125, 250, 500, 1000 μg/mL).

2.6.4. Analysis of gut microbiota during fecal fermentation

During fecal fermentation, the microbial composition of each group (NC, GOS-P, UPS) was analyzed at five different time points (0, 6, 12, 24, and 48 h). Genomic DNA was extracted using a Genomic DNA Kit from Tiangen in Beijing, China, and the V3-V4 regions of 16S rRNA were amplified and analyzed by BGI in Hong Kong. Library construction, concentration, and quality assessment were performed using Agencourt AMPure XP beads and Agilent 2100 Bioanalyzer. Next, the raw data was filtered using iTools Fqtools fqcheck (v.0.25), and the paired-end reads were merged into a single tag sequence using Fast Length Adjustment of SHort Reads (FLASH, v1.2.11). The sequences were then clustered into operational taxonomic units (OTUs) with a 97% similarity threshold by UPARSE, and chimeras were filtered using UCHIME (v4.2.40). The OTU representative sequences were mapped to the tags using USEARCH (v7.0.1090) and aligned against the database for taxonomic annotation using the RDP classifier (v2.2) at 60% sequence identity. To calculate alpha and beta diversity, we used mothur (v.1.31.2), QIIME (v1.80), and R (v3.1.1). Differential species analysis was carried out using Linear Discriminant Analysis Effect Size (LEfSe), while microbial functional annotation was predicted by PICRUSt2 v2.3.0-b and R (v3.4.10). Finally, correlation analysis and model prediction were performed using R (v3.4.1) and Cytoscape.

2.7. Statistical analyses

Experiments were conducted in triplicates, with purified UPS activities measured at concentrations ranging from 125 to 1000 μg/mL for statistical comparison. One-way and two-way ANOVA tests were carried out as needed using Minitab 19.0 (UAE University). Tukey's test was utilized to compare differences between the samples with a significance level of $P < 0.05$. Shimadzu LabSolutions software (Japan) was used for HPLC data analysis. All other software used has been appropriately cited within the text.

3. Results

3.1. Extraction of polysaccharides from date seeds

A CCD consisting of 26 runs, involving four independent variables at three different levels, was utilized to evaluate the individual and combined influences of these variables on the concentration of polysaccharides (PS). The optimization of the DES extraction parameters is delineated in Table S1. Subsequent data processing was executed using Design-Expert software, leading to developing a second-order polynomial regression model and the performance of ANOVA. The equation depicting the polysaccharides concentration (Y) (mg/mL) is as follows:

$$
\begin{aligned}
Y = {} & 0.143 + 0.2795\,A + 1.253\,B + 4.6215\,C - 6.6755\,D - 0.35775\,AB \\
& + 0.189\,AC + 0.025125\,AD + 0.11925\,BC - 1.446125\,BD \\
& - 4.053375\,CD + 0.464281\,A^2 + 1.283781\,B^2 - 0.580719\,C^2 \\
& + 2.564281\,D^2.
\end{aligned}
$$

In this model, the variables A, B, C, and D correspond to pH, time, solid-liquid ratio, and temperature, respectively. The quadratic (A^2, B^2, C^2, and D^2) and interaction terms (AB, AC, AD, BC, BD, CD) represent their respective squared and interactive effects on PS yield. The regression coefficients for each term in the model are listed in Table S2. The model's robustness is evidenced by a high F-value of 44.39. The coefficient of determination (R^2) value at 0.982611 implies that the model explains 98.26% of the variance for PS concentration. The

adjusted R^2 value at 0.96 corroborates the model's predictive capability, accounting for 96% of the variance. The *p*-values indicate the significance of the model terms, with values below 0.0001 highlighting the importance of the model, the main effects of factors B, C, and D, the quadratic influence of factor D, and the interactive influences of BD and CD.

Graphical representations of the optimization process for PS concentration *via* DES are depicted in Fig. S1 (A-F). The optimized factor levels achieving the highest extraction yield were found to be a pH of 4.30, a temperature of 70.0 °C, a solid-liquid ratio of 64.8 mg/mL, and a time duration of 82.2 min. Contrasting with these optimal conditions, empirical results indicated a superior concentration of PS at ~28.9 mg/mL when the extraction was conducted at pH 4.0, a duration of 120 min, a temperature of 100 °C, and a solid-liquid ratio of 10 mg/mL. These experimentally derived conditions were further employed for ultrasound-assisted extraction of DSP, examining the influence of ultrasound duration and amplitude on the concentration of ultrasound-processed polysaccharides (UPS).

Predictive modeling suggested a UPS concentration of about 28 mg/mL date seeds at 60 Pa of ultrasound amplitude and 20 min of processing. Corresponding empirical trials confirmed a slightly higher concentration of 34.4 mg/mL of PS, which was in close alignment with the predicted outcome, as documented in Table 2 (supplementary). RSM plots that illustrate the impact of ultrasonication on UPS concentration are showcased in Fig. S1G. Employing the fine-tuned extraction parameters, the polysaccharides were subsequently isolated and purified through TCA treatment, ethanol precipitation, and dialysis, culminating in a maximal concentration of 21.4 mg/mL of UPS, quantified by the phenol-sulfuric acid assay. The UPS was free from proteins, impurities, and low-molecular-weight substances. A fraction of this purified product was allocated for freeze-drying in preparation for additional characterization.

3.2. Characterization of UPS

UPS had an average Mw of ~3290.0 kDa, as shown in Fig. S1 A. Analysis of the monosaccharide composition of UPS, depicted in Fig. S2C and compared against PMP-derivatized monosaccharide standards (Fig. S2B), identified galactose as the predominant monosaccharide, succeeded by mannose, fructose, glucose, and galacturonic acid in descending order of concentration. FTIR spectroscopy analysis revealed that the UPS spectra (Fig. 1A) consisted of prominent absorption bands around 1022, 1441, 1522, 1618, and 3277 cm^{-1}, along with less intense bands in the regions of 550–906 cm^{-1}, 1980, and 2997 cm^{-1}. DSC results, presented as a temperature *versus* heat flow graph (Fig. 1B), showed that the glass transition of date seed polysaccharides commenced near 160 °C and concluded at 200 °C. Below this transition temperature, the polysaccharides were in a glassy state, characterized by considerable elasticity. These findings align with observations by Marouani et al. (2023), who reported a minor exothermic peak adjacent to the major endothermic dehydration peak, indicative of the decomposition of cellulose within the samples.

TGA provided insights into the thermal degradation pattern of UPS, illustrating the sample's thermal decomposition temperature, stability, and composition through a weight loss rate *versus* temperature plot (Fig. 1C). This analysis indicated an initial weight loss of 1% from 0 to 100 °C, followed by a 4% reduction in mass between 300 and 580 °C. Moreover, UPS presented a particle size of 3303.6 nm and a zeta potential of −421.92 mV. SEM revealed porous and irregular surface for UPS at various magnifications (250, 1000, 1500, and 3000×) in Fig. 2 (A-D). The dense, compact nature of the polysaccharides, uncharacteristic of typical polysaccharide structures, is likely attributed to the application of ultrasound during the extraction. Functional properties such as hydration and foaming are pivotal for the application of polysaccharides in food products. UPS demonstrated commendable water absorption, with a holding capacity of 2.9 ± 0.1 g/g, an oil retention ability of 6.4 ± 0.3 g/g, and a water solubility index of 82.9 ± 0.7%.

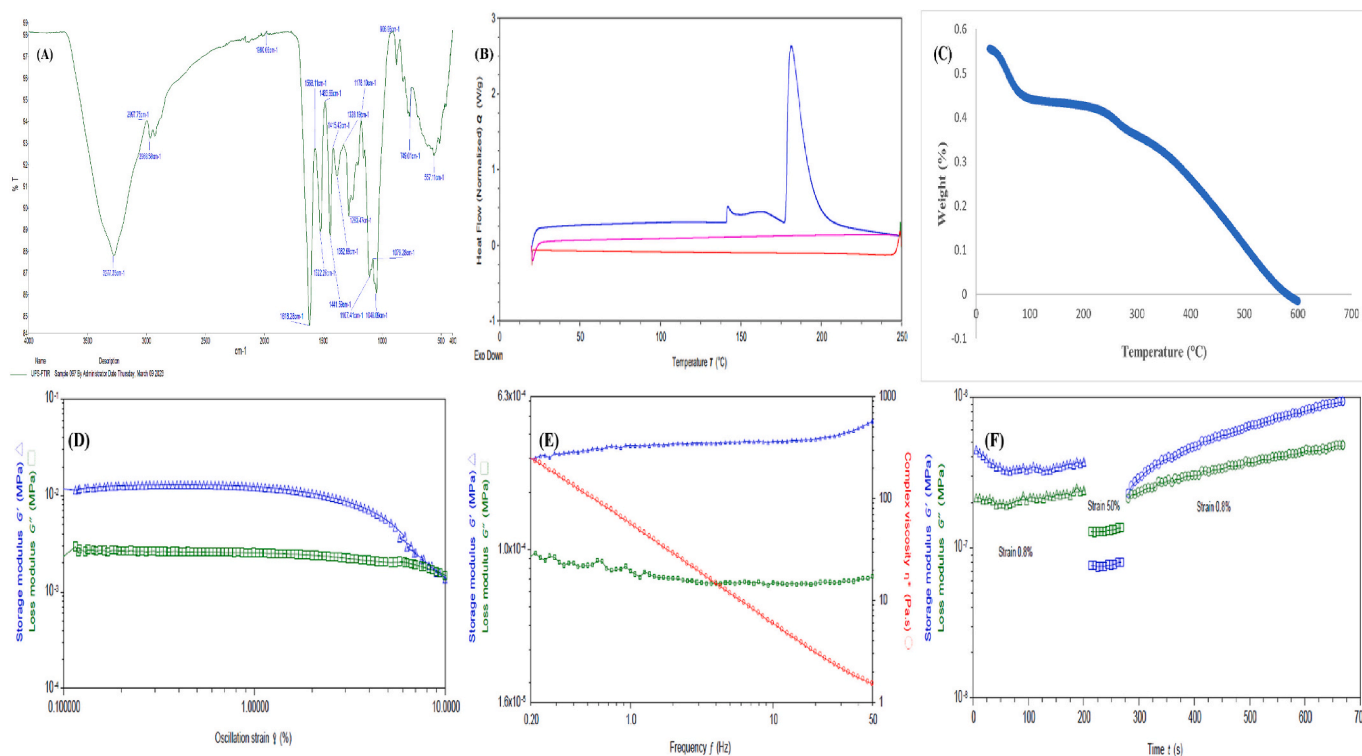Rheological measurements highlighted the viscoelastic

Fig. 1. Characterization of UPS including FTIR spectra (A); DSC curve (B); TGA (C); UPS storage and loss moduli amplitude sweep (D), frequency sweep (E), and time sweep (F) tests.
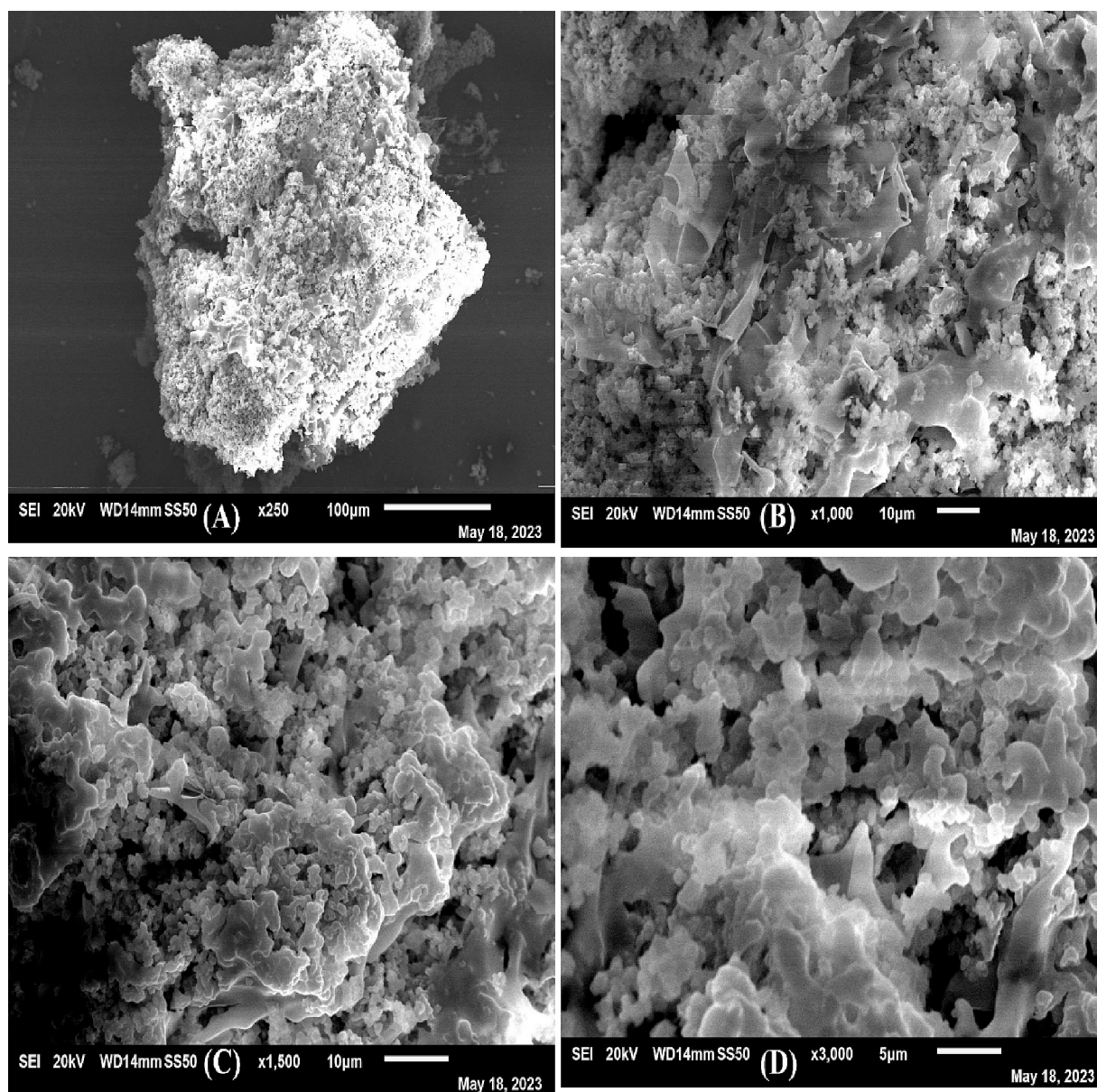
Fig. 2. SEM images of UPS, at magnifications corresponding to 250× (A), 1000× (B), 1500× (C), and 3000× (D).

characteristics of UPS, with the storage modulus (G') and loss modulus (G") assessed through various tests (Fig. 1D). Specifically, the G" value remained almost unchanged at approximately 10^{-3} MPa over an oscillation strain range of 0.1% to 10%, whereas G' demonstrated a decline from 10^{-2} to 10^{-3} MPa with increasing strain within this range, as seen in the amplitude sweep test (Fig. 1D). The intersection of the curves near

a 10% strain hinted at a threshold point. The dominance of G' over G" underlined the material's elastic behavior and its relatively lower viscosity. In the frequency sweep test, the G' of UPS showed an increase with frequency, indicating strong elastic characteristics, while G" stayed constant, regardless of frequency variations, as displayed in Fig. 1E. Conversely, the time sweep test exhibited a stable G' greater than G" at a

Table 1

In vitro antioxidant activities of UPS[1] at different concentrations.

UPS (µg/mL)	DPPH (%)	ABTS (%)	SAS (%)	SD (%)	HRS (%)	HP (%)	MC (µg/mL)	FRAP (µg/mL)	TAC (µg/mL)	RP (µg/mL)
125	23.1 ± 1.2^d	21.8 ± 0.1^d	24.8 ± 0.9^d	38.4 ± 0.1^d	33.4 ± 0.6^d	52.1 ± 0.1^d	1841.0 ± 129.2^d	111.6 ± 13.5^d	30.2 ± 1.3^d	32.8 ± 0.2^d
250	40.9 ± 0.9^c	39.9 ± 0.1^c	38.1 ± 0.3^c	49.1 ± 0.2^c	55.8 ± 0.7^c	60.2 ± 0.2^c	5642.9 ± 50.9^c	257.8 ± 25.1^c	192.4 ± 3.1^c	54.1 ± 2.8^c
500	57.4 ± 1.4^b	51.8 ± 0.2^b	48.3 ± 0.1^b	62.6 ± 0.4^b	61.1 ± 0.9^b	69.9 ± 0.1^b	7482.4 ± 31.9^b	441.1 ± 19.3^b	630.9 ± 27.1^b	159.9 ± 2.9^b
1000	61.9 ± 1.1^a	76.0 ± 0.1^a	64.3 ± 0.5^a	69.5 ± 0.2^a	79.2 ± 0.7^a	73.4 ± 0.2^a	$11,203.8 \pm 25.4^a$	627.4 ± 50.8^a	998.6 ± 113.4^a	353.8 ± 11.1^a

(a–d) Means of the values in the same column, but with different superscripts, are significantly different from each other (P < 0.05).

[1] Polysaccharide produced by ultrasound-assisted deep eutectic solvent extraction of date (*Phoenix dactylifera*) seeds. DPPH: 2,2-diphenyl-1-picrylhydrazyl; ABTS: 2,2′-azino-bis(3-ethylbenzothiazoline-6-sulfonic acid)); SAS: superoxide anion scavenging; SD: superoxide dismutase; HRS: hydroxy radical scavenging; HP: hydrogen peroxide scavenging; MC: metal chelating-; FRAP: ferric reducing antioxidant power; TAC: total antioxidant capacity; RP: reducing power.

0.8% strain for up to 200 s, after which G' slowly rose from 300 to 700 s (Fig. 1F). At a higher strain of 50%, G" overtook G' for about 100 s, suggesting a shift from an elastic to a more viscous state with the rise in applied strain.

3.3. Bioactivities of UPS

The antioxidant capacity of UPS was determined through a series of radical scavenging assays within a concentration range of 125–1000 µg/mL, detailed in Table 1. These assays measured the capacity of UPS to neutralize various free radicals, chelate metal ions, and reduce oxidants. An upward trend in radical scavenging was observed with increasing UPS concentrations, with DPPH and ABTS activities escalating from 23.1% to 61.9% and from 21.8% to 76%, respectively, when the concentration increased from 125 to 1000 µg/mL. Similarly, the superoxide dismutase-like activity and superoxide anion scavenging capacity of UPS rose from 38.4% to 69.5% and from 24.8% to 64.3%, respectively, as the concentration increased.

UPS's efficacy in scavenging ROS was assessed through hydrogen peroxide and hydroxyl radical scavenging assays. At a concentration of 1000 µg/mL, UPS achieved the highest scavenging activities of 73.4% for hydrogen peroxide and 79.2% for hydroxyl radicals. The metal ion chelation by UPS at 1000 µg/mL was 11,203.8 µg/mL, highlighting its antioxidant properties. Comparative analyses with standard ascorbic acid (1 mg/ml) through FRAP, TAC, and RP assays demonstrated that antioxidant potential increased with UPS concentration, reaching peaks of 627 µg/mL (FRAP), 998 µg/mL (TAC), and 353 µg/mL (RP) at 1000 µg/mL. The concentration-dependent increment in antioxidant properties of UPS was statistically significant ($P < 0.05$).

The antimicrobial efficacy of UPS against four prevalent foodborne pathogens was quantified at concentrations ranging from 1.33 to 10.7 mg/mL, with findings illustrated in Fig. S3. At the highest tested concentration (10.7 mg/mL), UPS inhibited *E. coli* O157:H7 by 60%, *S. aureus* by 66%, *S. typhimurium* by 69.7%, and L. *monocytogenes* by 50.2%. Inhibitory activities of UPS against α-glycosidase, α-amylase, and ACE are showcased in Fig. 3A. A significant augmentation in inhibition ($P < 0.05$) was recorded with rising UPS concentrations from 125 to 1000 µg/mL. The highest inhibition of α-glycosidase and α-amylase was at 1000 µg/mL, where UPS impeded these enzymes by 82% and 86%, respectively. ACE inhibition by UPS peaked at 68.4% at the same concentration, marginally lower than the inhibition rates of the other enzymes.

Detailed cytotoxic evaluations of UPS on Caco-2 and MCF-7 cell lines were conducted to ascertain its anticancer potential, as depicted in Fig. 3B. The results revealed a significant increase in inhibitory effect against Caco-2 cell lines at concentrations up to 500 µg/mL, beyond which the inhibition waned. Against MCF-7 cells, UPS maintained consistent inhibitory effects up to 500 µg/mL, followed by a decline, achieving 70% and 46% inhibition for Caco-2 and MCF-7 cell lines, respectively. Collectively, these findings endorse UPS as a promising bioactive polysaccharide source with considerable potential for application in the food sector and related industries.

3.4. In vitro digestion and prebiotic potential of UPS

The *in vitro* digestion study of UPS demonstrated a reduction in total sugars and an increment in reduced sugars post-digestion, as indicated in Fig. S4. Specifically, total sugar levels in UPS dipped from 33 to 15 mg/mL, while reduced sugar levels climbed from 1 to 7 mg/mL. The prebiotic capacity of UPS was further investigated through the growth kinetics of six probiotic strains utilizing UPS as a carbon source, with outcomes presented in Fig. S5. Each of the probiotic strains metabolized UPS comparably to glucose, underscoring the prebiotic capabilities of UPS. The initial lag phase of probiotic proliferation was almost identical for cultures grown on UPS and glucose. Nonetheless, UPS did not promote the exponential phase growth of L. *rhamnosus* and L. *gasseri* as effectively as glucose did.

3.5. In vitro fecal fermentation using UPS

3.5.1. In vitro fecal fermentation parameters

The *in vitro* impact of UPS on fecal fermentation was gauged by observing alterations in gas evolution, pH, sugar profiles, and SCFA generation, including acetic, propionic, and butyric acids, as depicted in Fig. 4A–4G. GOS-P and a blank devoid of carbohydrates served as the positive control and negative control (NC), respectively. The pH levels in the NC and GOS-P samples displayed a significant decline within the initial 12 h, followed by a rise peaking at 6.6 and 6.2, correspondingly (Fig. 2A). Conversely, UPS maintained a relatively steady pH throughout the fermentation process.

Gas production, indicated in Fig. 2B, demonstrated an increase from 0.5 to 2.5 within the first 24 h of fermentation for UPS, then tapered off to 0.75. The controls, GOS-P and NC exhibited a reduction in gas production post 12 h and a secondary rise at about 48 h. Total sugars diminished across all samples during fermentation, with UPS showing the lowest sugar content of 3.76 mg/mL at the 48-h mark, followed by NC and GOS-P (Fig. 2C). A significant variance in reducing sugars was also observed among the three groups throughout the fermentation
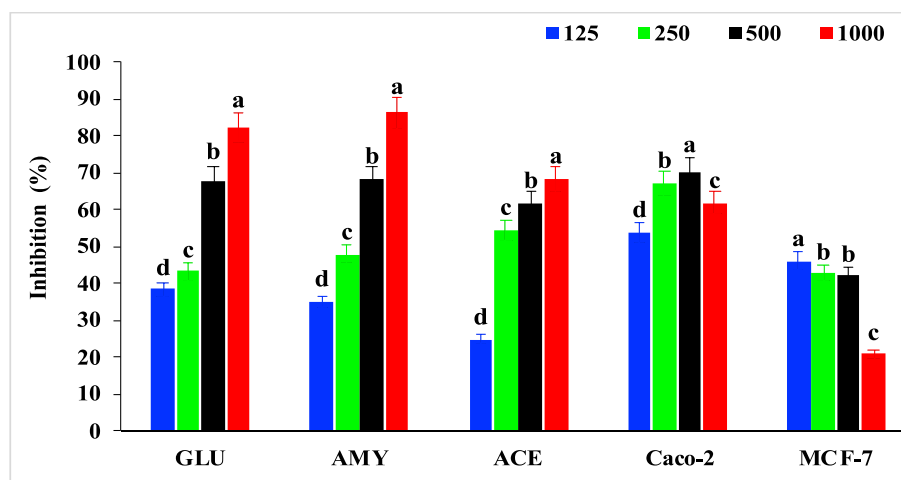

Fig. 3. *In vitro* bioactivities of UPS at different concentrations (µg/mL). GLU: α-glycosidase, AMY: α-amylase, ACE: angiotensin-converting enzyme, and anticancer activities against Caco-2 and MCF-7 cell lines of UPS. Bars are means ± standard deviations (error bars). [(a-d)] Means with different lowercase letters of the same parameter differed significantly ($P < 0.05$).
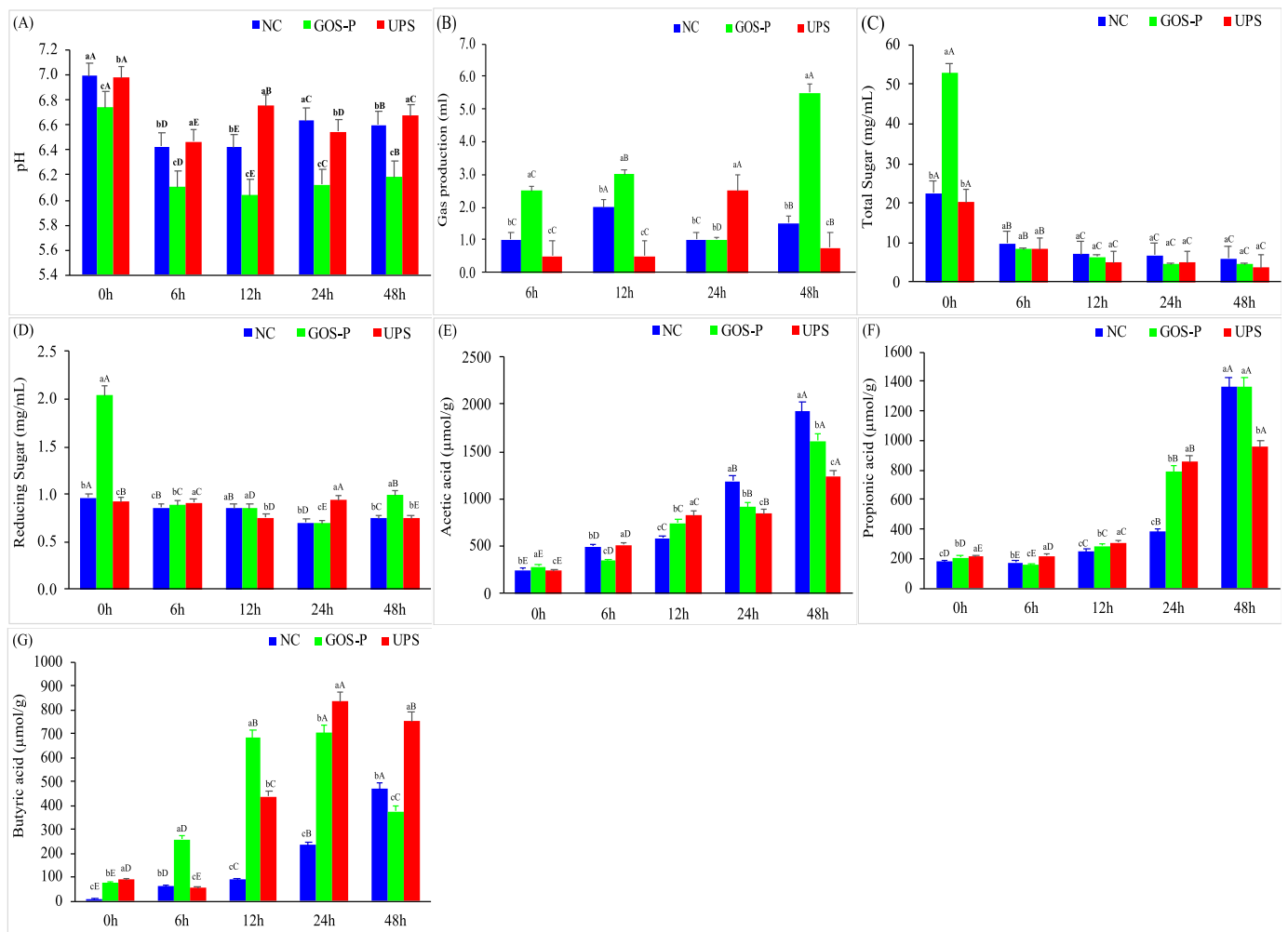
Fig. 4. Effect of UPS during 0, 6, 12, 24 and 48 h of fecal fermentation for pH (A), gas production (B), total sugar (C), reducing sugar (D), acetic acid production (E), propionic acid production (F), and butyric acid production (G) of the sample groups: NC (negative control), GOS-P (positive control) and UPS. Bars are means ± standard deviations (error bars). [a-d] indicates Means with different lowercase letters of same parameter differed significantly (P < 0.05). [A-D] Means with different uppercase letters differed significantly (P < 0.05).

duration (Fig. 2D). The concurrent decrease in pH, gas, and sugars, coupled with SCFA production, suggests effective UPS metabolism by the intestinal microbiota. Acetic, propionic, and butyric acids were the primary SCFAs detected, with their respective concentrations delineated in Fig. 2E-2G. At the end of 48 h, NC had the highest acetic acid levels (1362 μmol/g), trailed by GOS-P (1609 μmol/g) and UPS (1237 μmol/g) (Fig. 2(E)). Notably, the butyric acid levels from UPS (752 μmol/g) were superior to those in NC and GOS-P after 48 h of fermentation (Fig. 2G). Acid release from UPS initially diminished until 6 h but then ascended. Meanwhile, NC (1362 μmol/g) and GOS-P (1359 μmol/g) outperformed UPS (954 μmol/g) in propionic acid generation (Fig. 2F).

3.5.2. Effect of UPS on microbial and functional profile

The impact of purified UPS on gut microbiota and their functional profiles was rigorously analyzed. Utilizing a Venn diagram (Fig. 5A), the overlap and uniqueness of operational taxonomic units (OTUs) were determined across the three experimental sets: negative control (NC), GOS-P, and UPS. During *in vitro* fecal fermentation, there were 511 OTUs common to all groups. Notably, there were 96 OTUs overlapping between NC and GOS-P, 55 between GOS-P and UPS, and another 55 between NC and UPS, indicating a shared microbial presence between GOS-P and UPS. Uniquely, UPS supported the growth of 56 distinct OTUs, while the blank and GOS-P had 60 and 51 unique OTUs, respectively, suggesting that UPS enriches gut microflora comparably to the established positive control.

Alpha and beta diversity during fermentation are illustrated in Fig. 5B and Fig. S6, respectively. Alpha diversity, depicted through rarefaction indices and boxplots, considers observed species, Chao1, ACE, Shannon, Simpson, and coverage indices. Rarefaction curves (Fig. S5 (A-C)) show richness and diversity of the gut microbiota in GOS-P and UPS, while Fig. S5 (D–F) exhibits comparable diversity patterns across all groups. Alpha diversity box plots (Fig. 5 (B)) display variance in microbial diversity levels, with GOS-P manifesting the lowest diversity, followed by NC and UPS. To assess beta diversity, non-metric multidimensional scaling (NMDS), unweighted pair group method with arithmetic mean (UPGMA) clustering, and order abundance bar plots were conducted. The NMDS plot (Fig. 5C) delineates the distinct microbial communities among the groups across the fermentation timeline. The principal coordinate analysis (PCoA) diagram (Fig. 5D) further corroborates the distinctness of the enterotypes. Analysis of Bray-Curtis dissimilarity and relative abundance (Fig. 5E) highlighted that Enterobacteriales were predominantly abundant in UPS during fermentation. Other orders, such as Bifidobacteriales, Bacteroidales, Clostridiales, and Lactobacillales, were also profuse across all groups. A phylogenetic tree (Fig. 5F) supported these findings, identifying Firmicutes, Proteobacteria, Bacteroidetes, and Actinobacteria as the major phyla. Beta diversity insights concluded that UPS favored the presence of Enterobacteriales over Lactobacillales, unlike in the NC and GOS-P.
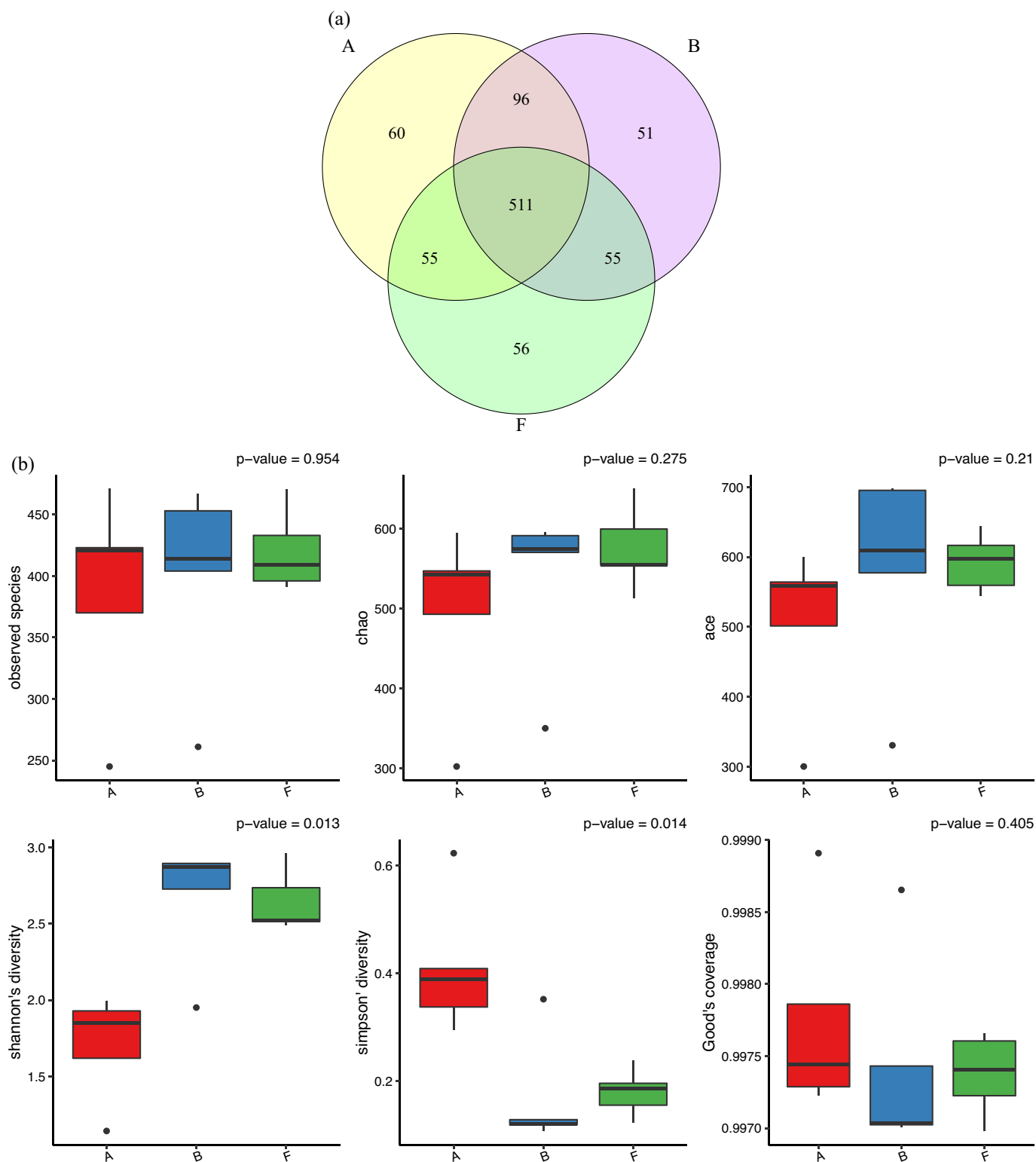
Fig. 5. Effect of UPS on gut microbiome composition during fecal fermentation. Venn diagram (A), box plot of different indices of alpha diversity (B), NMDS plot (C), PCoA plot (D), combination graph of UPGMA cluster tree and order abundance bar plot (E), and species phylogenetic analysis (F) of the sample groups, where A, B, and F are the sample groups: A- NC (negative control), B- GOS-P (positive control), and F-UPS.

Further investigations are warranted to discern whether UPS specifically enhances certain bacterial species within this phylum. Functional gene prediction of the gut microbiota was performed using PICRUSt2, referencing KEGG, COG, and MetaCyc databases to predict metabolic pathways.

At KEGG hierarchy level 1 (Fig. 6A), metabolic pathways were the most prevalent across all groups. At level 2 (Fig. 6B), pathways related to the metabolism of carbohydrates, energy, amino acids, terpenoids, polyketides, lipids, cofactors, and vitamins were notably active. Level 3 (Fig. 6C) detailed the pathways where UPS influenced the biosynthesis
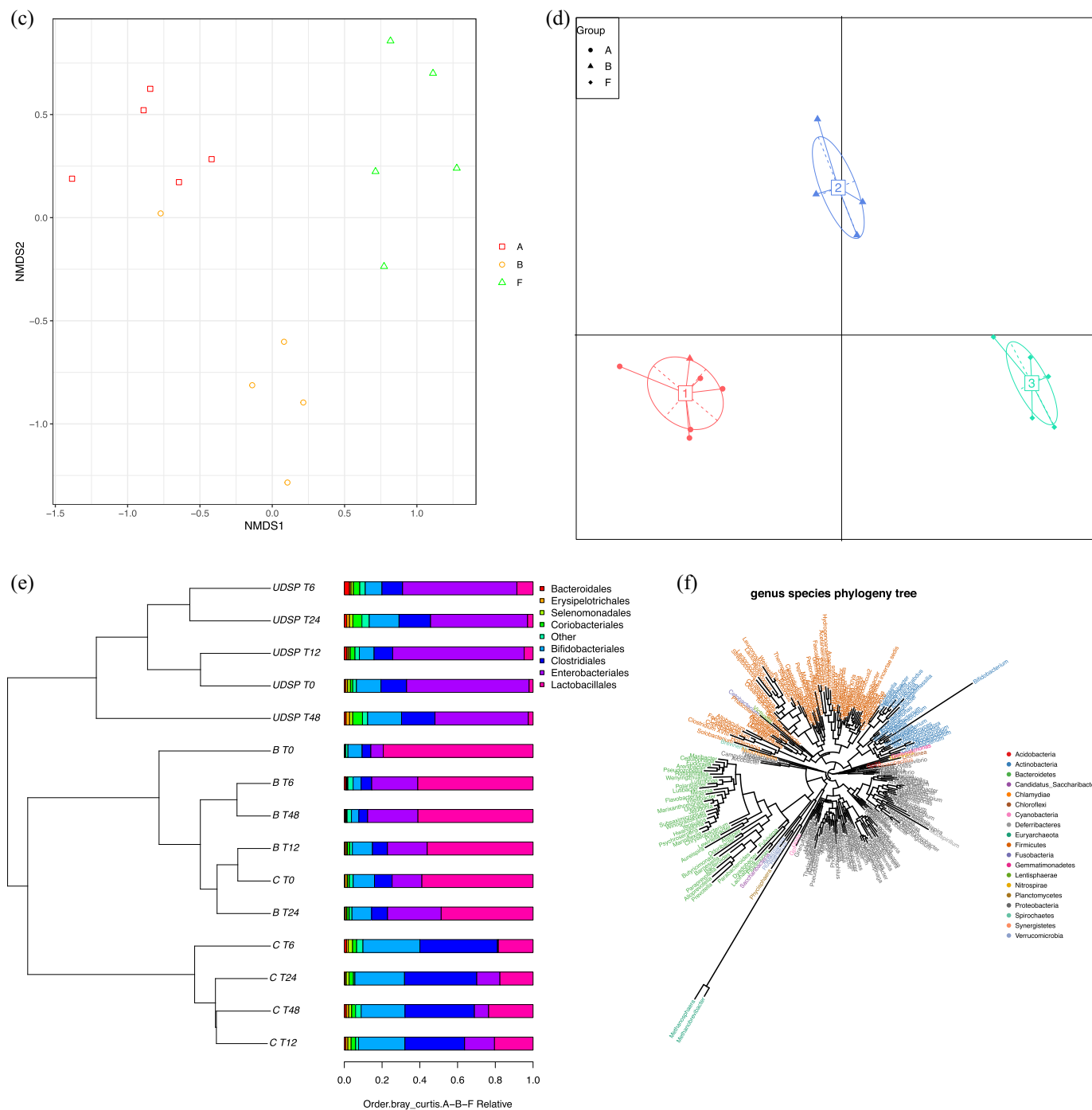
(c)

(d)

(e)

(f) genus species phylogeny tree

Fig. 5. (*continued*).

of ansamycins, primary bile acids, branched-chain amino acids, and the degradation of ethylbenzene. COG heatmap (Fig. 6(D)) affirmed these pathways, emphasizing functions associated with carbohydrate and amino acid transport and metabolism and translation ribosomal structure and biogenesis. The MetaCyc heatmap (Fig. 6E) aligned with these findings, showing abundant nucleoside, nucleotide, amino acid biosynthesis, and biosynthesis pathways for cofactors, prosthetic groups, electron carriers, and vitamins.

Species-specific interactions were explored through Spearman correlation analysis and network analysis, identifying relationships among various species in the fecal microbiota (Fig. 6F). *Bifidobacterium longum* showed strong positive correlations with *Blautia luti*, *Blautia schinkii*, and positive correlations with *Blautia wexlerae* and *Romboutsia sedimentorum*.

Escherichia and *Enterococcus saccharolyticus* demonstrated strong negative correlations with the rest of the microbial diversity. Network analysis (Fig. S7A) identified a positive correlation between *Enterococcus saccharolyticus* and most other microbial species. Finally, relative abundance heatmaps (Fig. S7B and S7C) indicated the dominance of Firmicutes in NC and GOS-P, with a higher prevalence of Proteobacteria in UPS.

4. Discussions

The application of ultrasound in the extraction of bioactive compounds from natural matrices is predicated on the disruptive capabilities of low-frequency, high-power ultrasound waves to cellular walls. This

Fig. 6. Effect of UPS on different microbial functions during fecal fermentation. Histograms of KEGG pathways abundance at levels 1–3 (A-C), heatmap of COG pathways (D), heatmap of MetaCyc pathways (E), and species spearman coefficients analysis of OTUs in each sample group (F), where A, B, and F are the sample groups: A- NC (negative control), B- GOS-P (positive control), and F-UPS.

sonication process facilitates the release of the encapsulated analytes and enhances their mass transfer by improving solvent penetration into the matrix. Dhahri et al. (2023) yielded a 1.03% extraction rate of Ajwa date seed polysaccharide *via* ultrasound-assisted hot water extraction, whereas (Noorbakhsh & Khorasgani, 2023) reported PS yield of 17.52 g/ 100 g *via* ultrasound-assisted alkaline hot water extraction. Our previous study has reported PS yield of 42.135 mg/g (Subhash et al., 2024) when coupling DES extraction with microwave processing. Adopting eco-friendly solvents in conjunction with non-thermal extraction methods has been implicated in the substantial increase in yield observed in this experiment. Furthermore, the thermal dynamics induced by ultrasound exposure favorably impact the solubility of bioactive entities such as polysaccharides. Initially, the ultrasonic waves catalyze the rapid disruption of cell walls, which, in conjunction with the vibratory motion that induces cavitation, results in the efficient release of polysaccharides

for extraction (Wang, Xiong, & Huang, 2023). Therefore, the deep eutectic solvent (DES) extraction assisted by ultrasound has been successful in extracting ultrasonically processed polysaccharides (UPS) by disassociating noncovalent intra- and inter-molecular interactions, thereby mobilizing water-soluble polysaccharide fractions.

The ultrasound process exerts an influence on the molecular weight, monosaccharide profile, and structural integrity of the polysaccharides (Wang et al., 2023). In our investigation, galactose was identified as the predominant monosaccharide component. Variability in the monosaccharide composition of date seed polysaccharides across different studies can be attributed to the disparities in source materials, extraction parameters, and the methodologies employed (Noorbakhsh & Khorasgani, 2023). Mannose, glucose, xylose, and arabinose were the principal monosaccharides in Ajwa date seeds, with xylose and arabinose present in the date flesh. Our findings concur with Dhahri et al. (2023),
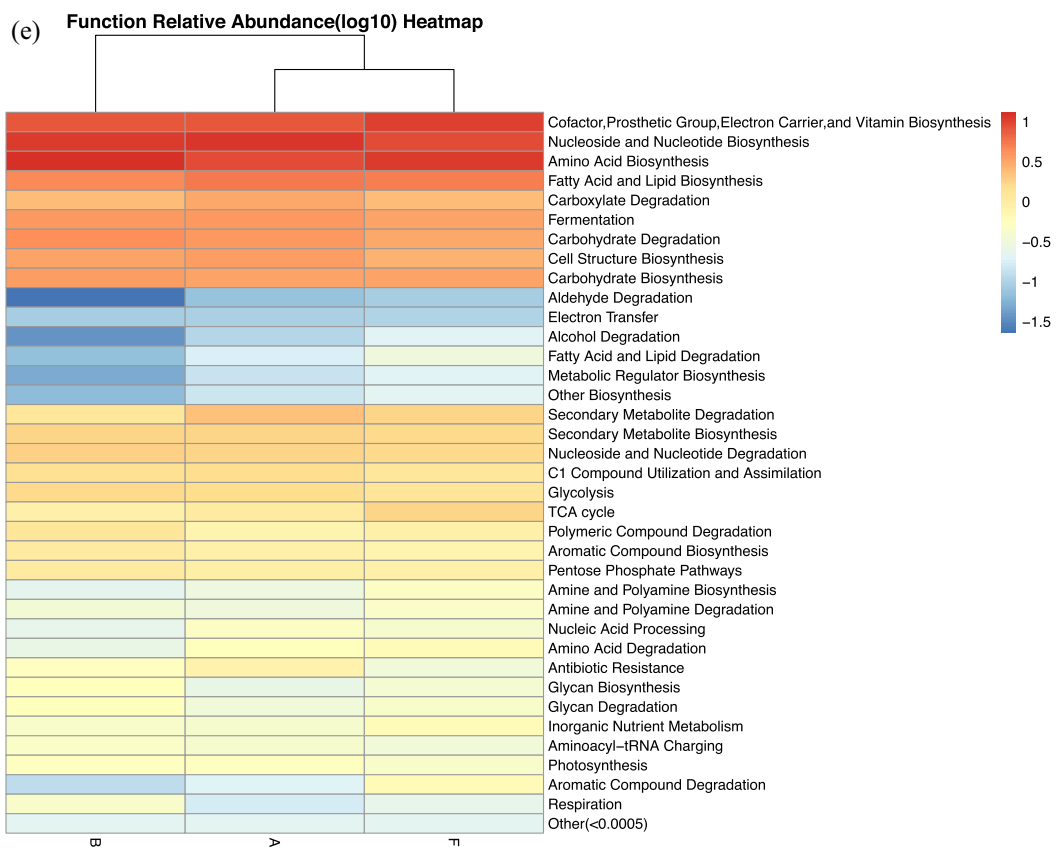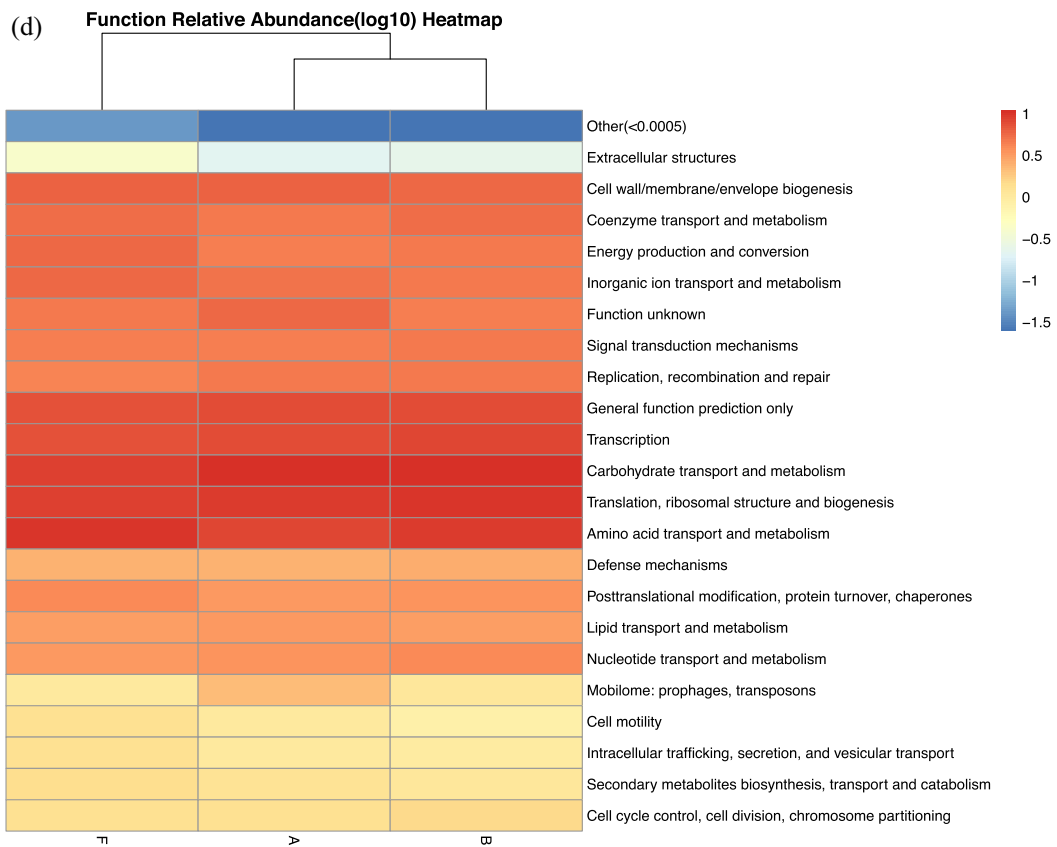
(d)

Function Relative Abundance(log10) Heatmap

(e)

Function Relative Abundance(log10) Heatmap
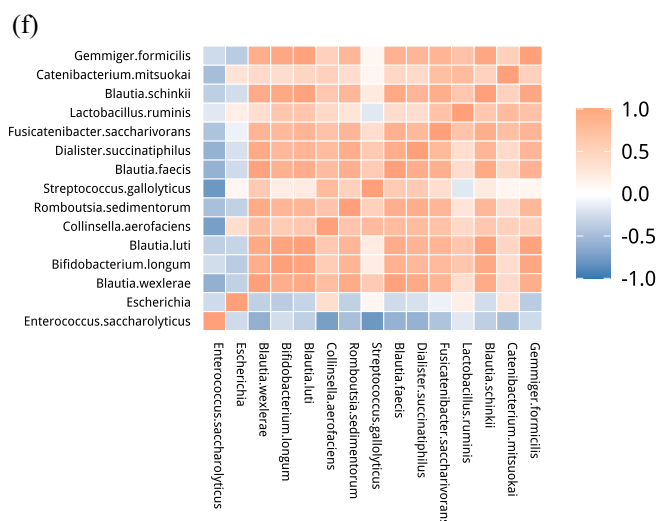

Fig. 6. (*continued*).

(f)

Fig. 6. (*continued*).

noting minimal or absent peaks for xylose and arabinose in the seed polysaccharides extracted using ultrasound, thereby confirming the consistency of our results. The molecular weight spectrum of UPS revealed multiple absorption peaks, suggesting that UPS is a hetero-polysaccharide characterized by a diverse range of molecular weights, similar to the polysaccharides found in jujuba seeds (Li et al., 2019).

The FTIR spectral analysis of UPS (Fig. 1A) presents broad absorption bands at approximately 1022 cm^{-1} and 3277 cm^{-1}, corresponding to the C—O stretching vibrations associated with cellulose and the O—H stretching of both cellulose and water within the polysaccharide. The prominent peaks around 1441 and 1616 cm^{-1} are indicative of the C═C skeletal vibrations characteristic of lignin and hemicellulose, and the C—O stretching vibrations in cellulose. The less intense absorption peaks at 2997 cm^{-1} are suggestive of the C—H stretching vibrations typical of polysaccharides (Noorbakhsh & Khorasgani, 2023). Additionally, absorption bands at 1382 and 1415 cm^-1 align with the O–C═O bending vibrations of uronic acids present in the date seeds, corroborating the FTIR spectra characteristics of polysaccharides from Ajwa date seeds as described by Dhahri et al. (2023).

The TGA curve of UPS delineates a distinct degradation profile that follows an exothermic pattern, evidenced by a marked mass loss upon reaching 200 °C, consistent with findings on date seed pyrolysis (Babiker, Aziz, Heikal, & Yusup, 2013). The inflection observed in the TG curve between 120 and 410 °C can be attributed to the thermal decomposition of date seed constituents such as hemicelluloses, cellulose, and lignin. A broad endothermic peak extending from 200 to 580 °C may correspond to the decomposition of lignin, a significant constituent of dietary fiber in date fruits (Babiker et al., 2013).

The water-holding capacity of polysaccharides is integral to food preparation, significantly affecting both functionality and sensory qualities. The oil-holding capacity is equally critical, influencing mouthfeel, texture, and flavor profiles in food products. Our results indicate that UPS possesses an impressive water solubility index, alongside significant oil and water retention capabilities. These properties affirm that hydrophilic substances, such as polysaccharides, characteristically exhibit superior water solubility and retention capacities. The findings are in line with those reported by Noorbakhsh and Khorasgani (2023), suggesting that polysaccharides with enhanced water-holding capacity, such as UPS, may facilitate stool bulking, potentially mitigating constipation and inflammation while promoting the elimination of free radicals.

Rheological assessments are vital to understand the flow properties of polysaccharides, offering insights into textural, compositional, and structural modifications that might occur throughout various stages of food processing, packaging, and storage. The storage modulus (G') and loss modulus (G") are indicative of the solid-like and liquid-like behaviors, respectively. Frequency sweep tests of UPS revealed a dominant G' over G", without any intersections, signifying pronounced elasticity—a characteristic potentially indicative of gelation properties of the polysaccharide. These rheological properties are consistent with the observations of Niknam, Mousavi, and Kiani (2020), which reported significant solid-like elastic properties where the storage modulus prevailed over the loss modulus.

Antioxidants, a critical category of bioactive components, play a protective role against cellular stress induced by free radicals, thereby forestalling oxidative damage and the onset of various diseases (Dhahri et al., 2023; Gulcin, 2020; Gülçin, 2012). UPS demonstrated considerable radical scavenging activity, corroborating the trends observed (Dhahri et al., 2023; Noorbakhsh & Khorasgani, 2023) in polysaccharides extracted through both hot water and ultrasound-assisted methods at elevated concentrations. The radical scavenging aptitude of polysaccharides is attributed to the molecular structure, inclusive of monosaccharide constituents, glycosidic linkages, and functional groups such as carbonyl and amino groups within the polysaccharide framework (Mohammed et al., 2021). The pronounced presence of carbonyl and carboxyl functionalities in date seed polysaccharides, in conjunction with phenolic compounds within the seeds, may elucidate the observed augmented antioxidant capacity (Noorbakhsh & Khorasgani, 2023). Comparable activities in superoxide dismutase-like and superoxide anion radical scavenging were observed in polysaccharides from Radix Cyathulae officinalis Kuan, with peak activities at a polysaccharide concentration of 1 mg/mL (Han et al., 2015). Moreover, UPS activities such as hydrogen peroxide scavenging, hydroxyl radical neutralization, and metal ion chelation exhibited a dose-dependent escalation, potentially due to cross-linking interactions between carboxyl groups of the galacturonic acid units and divalent metal ions (Lin, Wang, Chang, Inbaraj, & Chen, 2009). UPS also demonstrated cytotoxicity against MCF-7 and Caco-2 cell lines, suggesting potential anticancer properties. Additionally, the inhibition of enzymes associated with diabetes by UPS suggests its potential as an antidiabetic agent. The ACE inhibition activity of UPS points to its significant antihypertensive effects, aligning with literature on seed polysaccharides Sorourian, Khajehrahimi, Tadayoni, Azizi, and Hojjati (2022). The antibacterial efficacy of polysaccharides is influenced by the extraction methodology and the structural characteristics of the polysaccharides, with differential interactions noted between gram-negative and gram-positive bacteria due to their distinct cell wall compositions (Noorbakhsh & Khorasgani, 2023).

In vitro digestion studies on UPS suggest it undergoes partial degradation, yielding reducing sugars at the conclusion of the digestive process. The hydrolysis of glycosidic bonds, exposing reducing ends, and the concomitant liberation of sugars, provides a plausible mechanism for this observation. It is noteworthy that UPS, synthesized *via* ultrasound-facilitated DES extraction, displayed superior antioxidant and antimicrobial properties compared to extracts obtained using conventional organic solvents (Boudghane et al., 2023). Reports by Han et al. (2022) have shown a parallel increase in reducing sugar content in *Ziziphus Jujuba* polysaccharides post-digestion, mirroring the behavior of UPS. The resistance of polysaccharides to gastrointestinal enzymes is a defining feature of prebiotics. As such, polysaccharides that are indigestible or only partially digestible are likely to be metabolized by gut microbiota, yielding reducing sugars that serve as nutritive substrates for the resident gut flora. The prebiotic potential of UPS, facilitating the proliferation of probiotics, was evidenced in its capacity to promote the growth of standard Lactobacillus strains, resonating with prior studies on date seed polysaccharides (Al-Thubiani & Ahmad Khan, 2017). The gradual breakdown of UPS to monosaccharides enhances microbial growth by providing a carbon source.

The fermentation of UPS by gut microbiota led to a reduction in pH and an uptick in gas production from 6 to 24 h, as similarly documented by Van den Abbeele et al. (2020). The initial rise in gas production can be ascribed to the microbial catabolism of undigested food residues. A pronounced drop in pH following 6 h of fermentation across all samples suggests the conversion of sugars into their acidic counterparts. This acidic milieu aids in warding off pathogenic gut inhabitants by fostering a selective microbiota ecosystem, thereby bolstering gastrointestinal health. The fermentation of polysaccharides acidifies the intestinal environment, catalyzing the synthesis of SCFAs, which are integral to host metabolism, the integrity of the intestinal epithelial barrier, and protection against gastrointestinal disorders (Zeyneb et al., 2021). The predominance of SCFAs like acetic, propionic, and butyric acids contribute to the rapid acidification of the fecal broth. Our findings show that UPS promotes a greater release of acetic acid compared to NC and GOS-P, indicative of the presence of Bifidobacterium and Lactobacillus species, corroborating the results of Wu et al. (2021). The SCFA profile during fecal fermentation complements the demonstrated prebiotic effect of UPS on select probiotics (Fig. S5), wherein UPS was efficiently utilized as a carbohydrate source. UPS's performance mirrored that of the established prebiotic GOS-P, positing UPS as a promising functional prebiotic component. The SCFAs generated from UPS fermentation contribute to pH reduction, enhanced mineral bioavailability, and selective promotion of beneficial gut microbiota. The microbial preference for butyric acid followed by propionic acid as an energy source is well-documented (Zeyneb et al., 2021).

Our analyses have confirmed the presence of microbial genera implicated in SCFA production, notably Bifidobacterium, known for acetic acid synthesis, and Clostridium, which plays a role in the equilibrium of gut microbiota (Yi et al., 2022). Gut microbiota orchestrates critical functions related to energy metabolism and immunological response. Dietary fibers, such as polysaccharides, modulate gut microbiota composition, thus imparting health benefits to the host (Wu et al., 2021). It is imperative to elucidate the interactions between polysaccharides and the gut microbiota. Bacteroidetes, identified as the second predominant phylum, constitute the primary gut bacteria engaged in polysaccharide degradation. Similar to quinoa polysaccharides, which are substrates for Bacteroidetes growth, ultrasound-modified polysaccharides have been reported to influence the proliferation of Lactobacillus and Bacteroidaceae, in addition to SCFA production Hu, Nie, Li, Wang, and Xie (2018).

The acidified fecal milieu, characterized by low pH, was conducive to the growth of Firmicutes, known for butyrate production, while restraining the proliferation of Bacteroides. Spearman correlation analysis at the species level disclosed a robust positive association between the growth of Bifidobacterium and Blautia, an organism integral

to the conversion of dietary cellulose into SCFAs (Fan et al., 2020). The heatmap analyses of phyla and species revealed an abundance of Firmicutes in the NC and GOS-P samples and Proteobacteria in the UPS, aligning with the findings of Wu et al. (2021). These taxa are commonly involved in dietary fiber breakdown, SCFA release, energy extraction, and the reduction of obesity risk (Han et al., 2022). In summation, UPS has been shown to foster a rich diversity of microbiota and enhance biodiversity, mitigating the expansion of Firmicutes and promoting the growth of the Bacteroidetes phylum more effectively than the control. The observed relative abundance of beneficial genera suggests that UPS holds the potential to support the maintenance of the intestinal epithelium.

5. Conclusions

Polysaccharides synthesized *via* DES extraction exhibited heterogeneity in molecular weight profiles and monosaccharide composition, indicative of their heteropolysaccharide nature. These compounds demonstrated significant bioactivity, manifesting in potent antioxidant, anticancer, antidiabetic, antihypertensive, and antimicrobial properties, which were observed to intensify concentration-dependent. Additionally, the current polysaccharides possess prebiotic qualities that aid in the development of beneficial probiotic bacteria, thus could by employed as functional ingredients in food products. Furthermore, their rheological and functional attributes indicate their potential utility as gelation agents for various food products, particularly dairy products. This presents a vast array of possibilities for the implementation of these compounds. *In vitro* digestion studies were conducted to investigate the digestive resilience and biotransformation of these polysaccharides within the gastrointestinal milieu. This current study revealed that the UPS exerts a beneficial effect on the gut microbiota, enhancing microbial growth during *in vitro* fecal fermentation. This interaction culminated in the generation of SCFAs, contributing to an improved metabolic profile and indicative of the functional potential of these biopolymers in gut health modulation.

CRediT authorship contribution statement

Athira Jayasree Subhash: Writing – original draft, Visualization, Investigation, Formal analysis, Data curation. **Gafar Babatunde Bamigbade:** Writing – review & editing, Investigation. **Mohammed Tarique:** Investigation. **Basel Al-Ramadi:** Writing – review & editing, Supervision. **Basim Abu-Jdayil:** Writing – review & editing, Supervision. **Afaf Kamal-Eldin:** Writing – review & editing, Conceptualization. **Laura Nyström:** Writing – review & editing, Conceptualization. **Mutamed Ayyash:** Writing – review & editing, Validation, Supervision, Software, Resources, Project administration, Funding acquisition, Data curation, Conceptualization.

Declaration of competing interest

The authors declare that they have no known competing financial interests or personal relationships that could have appeared to influence the work reported in this paper.

Data availability

Data will be made available on request.

Acknowledgment

Appendix A. Supplementary data

Supplementary data to this article can be found online at https://doi.org/10.1016/j.fochx.2024.101354.

References

Al-Farsi, M. A., & Lee, C. Y. (2011). Usage of date (Phoenix dactylifera L.) seeds in human health and animal feed. In *Nuts and seeds in health and disease prevention* (pp. 447–452). Elsevier. https://doi.org/10.1016/B978-0-12-375688-6.10053-2.

Al-Hamayda, A., Abu-Jdayil, B., & Ayyash, M. (2023). Utilizing date pits in microencapsulation: Effect of different variations on probiotic survivability under in-vitro digestion. *LWT, 114917.* https://doi.org/10.1016/j.lwt.2023.114917

Al-Nabulsi, A. A., Jaradat, Z. W., Al Qudsi, F. R., Elsalem, L., Osaili, T. M., Olaimat, A. N., … Ayyash, M. M. (2022). Characterization and bioactive properties of exopolysaccharides produced by Streptococcus thermophilus and Lactobacillus bulgaricus isolated from labaneh. *LWT, 167,* Article 113817. https://doi.org/10.1016/j.lwt.2022.113817

Al-Thubiani, A. S., & Ahmad Khan, M. S. (2017). The prebiotic properties of date palm (Phoenix dactylifera L.) seeds in stimulating probiotic Lactobacillus. *Journal of Pure & Applied Microbiology, 11*(4). https://doi.org/10.22207/JPAM.11.4.05

Ayyash, M., Abdalla, A., Alhammadi, A., Senaka Ranadheera, C., Affan Baig, M., Al-Ramadi, B., Chen, G., Kamal-Eldin, A., & Huppertz, T. (2021). Probiotic survival, biological functionality and untargeted metabolomics of the bioaccessible compounds in fermented camel and bovine milk after in vitro digestion. *Food Chemistry, 363,* Article 130243. https://doi.org/10.1016/j.foodchem.2021.130243

Ayyash, M., Al-Nuaimi, A. K., Al-Mahadin, S., & Liu, S.-Q. (2018). In vitro investigation of anticancer and ACE-inhibiting activity, α-amylase and α-glucosidase inhibition, and antioxidant activity of camel milk fermented with camel milk probiotic: A comparative study with fermented bovine milk. *Food Chemistry, 239,* 588–597. https://doi.org/10.1016/j.foodchem.2017.06.149

Ayyash, M., Stathopoulos, C., Abu-Jdayil, B., Esposito, G., Baig, M., Turner, M. S., … Osaili, T. (2020). Exopolysaccharide produced by potential probiotic enterococcus faecium MS79: Characterization, bioactivities and rheological properties influenced by salt and pH. *LWT, 131,* Article 109741. https://doi.org/10.1016/j.lwt.2020.109741

Babiker, M. E., Aziz, A. R. A., Heikal, M., & Yusup, S. (2013). Pyrolysis characteristics of phoenix dactylifera date palm seeds using thermo-gravimetric analysis (TGA). *International Journal of Environmental Science and Development, 521-524.* https://doi.org/10.7763/IJESD.2013.V4.406

Barakat, A. Z., Hamed, A. R., Bassuiny, R. I., Abdel-Aty, A. M., & Mohamed, S. A. (2020). Date palm and saw palmetto seeds functional properties: Antioxidant, anti-inflammatory and antimicrobial activities. *Journal of Food Measurement and Characterization, 14*(2), 1064–1072. https://doi.org/10.1007/s11694-019-00356-5

Bouaziz, F., Ben Abdeddayem, A., Koubaa, M., Ellouz Ghorbel, R., & Ellouz Chaabouni, S. (2020). Date seeds as a natural source of dietary fibers to improve texture and sensory properties of wheat bread. *Foods, 9*(6). https://doi.org/10.3390/foods9060737

Boudghane, L. C., Bouabdellah, N., Bouanane, S., Ahmed, F. Z. B., Laroussi, M. A., Bendiaf, Y., … Merzouk, H. (2023). Phytochemical, antioxidant, and antimicrobial attributes of different extracts of seeds: The Algerian variety of dates 'Deglet Nour' (*Phoenix dactylifera* L.). *Vegetos, 36*(2), 559–565. https://doi.org/10.1007/s42535-022-00413-3

Dhahri, M., Sioud, S., Alsuhaymi, S., Almulhim, F., Haneef, A., Saoudi, A., … Emwas, A.-H. M. (2023). Extraction, characterization, and antioxidant activity of polysaccharides from ajwa seed and flesh. *Separations, 10*(2). https://doi.org/10.3390/separations10020103

Dobrowolska-Iwanek, J., Lauterbach, R., Huras, H., Paśko, P., Prochownik, E., Woźniakiewicz, M., Chrząszcz, S., & Zagrodzki, P. (2020). HPLC-DAD method for the quantitative determination of short-chain fatty acids in meconium samples. *Microchemical Journal, 155,* Article 104671. https://doi.org/10.1016/j.microc.2020.104671

DuBois, M., Gilles, K. A., Hamilton, J. K., Rebers, P. T., & Smith, F. (1956). Colorimetric method for determination of sugars and related substances. *Analytical Chemistry, 28* (3), 350–356. https://doi.org/10.1021/ac60111a017

El Sheikh, D. M., El-Kholany, E. A., & Kamel, S. M. (2014). Nutritional value, cytotoxicity, anti-carcinogenic and beverage evaluation of roasted date pits. *World Journal of Dairy & Food Sciences, 9*(2), 308–316. https://doi.org/10.5829/idosi.wjdfs.2014.9.2.91144

Fan, Q., Jiang, C., Wang, W., Bai, L., Chen, H., Yang, H., Wei, D., & Yang, L. (2020). Eco-friendly extraction of cellulose nanocrystals from grape pomace and construction of self-healing nanocomposite hydrogels. *Cellulose, 27*(5), 2541–2553. https://doi.org/10.1007/s10570-020-02977-2

FAOSTAT. (2023). *Food and agriculture organization statistics (FAOSTAT). Food and agriculture Organization of the United Nations.* Retrieved 02 Feb 2024 from https://www.fao.org/faostat/en/#data.

Gao, C., Cai, C., Liu, J., Wang, Y., Chen, Y., Wang, L., & Tan, Z. (2020). Extraction and preliminary purification of polysaccharides from Camellia oleifera Abel. Seed cake using a thermoseparating aqueous two-phase system based on EOPO copolymer and deep eutectic solvents. *Food Chemistry, 313,* Article 126164. https://doi.org/10.1016/j.foodchem.2020.126164

Ghnimi, S., Umer, S., Karim, A., & Kamal-Eldin, A. (2017). Date fruit (Phoenix dactylifera L.): An underutilized food seeking industrial valorization. *NFS Journal, 6,* 1–10. https://doi.org/10.1016/j.nfs.2016.12.001

Gülçin, İ. (2012). Antioxidant activity of food constituents: An overview. *Archives of Toxicology, 86*(3), 345–391. https://doi.org/10.1007/s00204-011-0774-2

Gulcin, İ. (2020). Antioxidants and antioxidant methods: An updated overview. *Archives of Toxicology, 94*(3), 651–715. https://doi.org/10.1007/s00204-020-02689-3

Gulcin, İ., & Alwasel, S. H. (2022). Metal ions, metal chelators and metal chelating assay as antioxidant method. *Processes, 10*(1), 132. https://www.mdpi.com/2227-9717/10/1/132.

Gulcin, İ., & Alwasel, S. H. (2023). DPPH radical scavenging assay. *Processes, 11*(8), 2248. https://www.mdpi.com/2227-9717/11/8/2248.

Han, X., Shen, S., Liu, T., Du, X., Cao, X., Feng, H., & Zeng, X. (2015). Characterization and antioxidant activities of the polysaccharides from Radix Cyathulae officinalis Kuan. *International Journal of Biological Macromolecules, 72,* 544–552. https://doi.org/10.1016/j.ijbiomac.2014.09.007

Han, X., Zhou, Q., Gao, Z., Lin, X., Zhou, K., Chitrakar, B., Chen, H., & Zhao, W. (2022). In vitro digestion and fecal fermentation behaviors of polysaccharides from Ziziphus Jujuba cv. Pozao and its interaction with human gut microbiota. *Food Research International, 162,* Article 112022. https://doi.org/10.1016/j.foodres.2022.112022

Ho Do, M., Seo, Y. S., & Park, H.-Y. (2021). Polysaccharides: Bowel health and gut microbiota. *Critical Reviews in Food Science and Nutrition, 61*(7), 1212–1224. https://doi.org/10.1080/10408398.2020.1755949

Hu, J.-L., Nie, S.-P., Li, C., Wang, S., & Xie, M.-Y. (2018). Ultrasonic irradiation induces degradation and improves prebiotic properties of polysaccharide from seeds of Plantago asiatica L. during in vitro fermentation by human fecal microbiota. *Food Hydrocolloids, 76,* 60–66. https://doi.org/10.1016/j.foodhyd.2017.06.009

Huang, Y., Feng, F., Jiang, J., Qiao, Y., Wu, T., Voglmeir, J., & Chen, Z. G. (2017). Green and efficient extraction of rutin from tartary buckwheat hull by using natural deep eutectic solvents. *Food Chemistry, 221,* 1400–1405. https://doi.org/10.1016/j.foodchem.2016.11.013

Ishrud, O., Zahid, M., Zhou, H., & Pan, Y. (2001). A water-soluble galactomannan from the seeds of Phoenix dactylifera L. *Carbohydrate Research, 335*(4), 297–301. https://doi.org/10.1016/S0008-6215(01)00245-2

Jiang, L., Ren, Y., Shen, M., Zhang, J., Yu, Q., Chen, Y., Zhang, H., & Xie, J. (2021). Effect of acid/alkali shifting on function, gelation properties, and microstructure of Mesona chinensis polysaccharide-whey protein isolate gels. *Food Hydrocolloids, 117,* Article 106699. https://doi.org/10.1016/j.foodhyd.2021.106699

Li, J. H., Li, W., Luo, S., Ma, C. H., & Liu, S. X. (2019). Alternate ultrasound/microwave digestion for deep eutectic hydro-distillation extraction of essential oil and polysaccharide from Schisandra chinensis (Turcz.) Baill. *Molecules, 24*(7). https://doi.org/10.3390/molecules24071288

Lin, C. L., Wang, C. C., Chang, S. C., Inbaraj, B. S., & Chen, B. H. (2009). Antioxidative activity of polysaccharide fractions isolated from Lycium barbarum Linnaeus. *International Journal of Biological Macromolecules, 45*(2), 146–151. https://doi.org/10.1016/j.ijbiomac.2009.04.014

Marouani, M. E., El Hamdaoui, L., Boulhaoua, M., Pienaar, A., Trif, L., Costa, G., … Kifani-Sahban, F. (2023). Non-isothermal kinetics of phoenix dactylifera L. date palm seeds pyrolysis using model fitting and Iso-conversional model free methods. *ChemistrySelect, 8*(11). https://doi.org/10.1002/slct.202203946

Mohammed, A. S. A., Naveed, M., & Jost, N. (2021). Polysaccharides; classification, chemical properties, and future perspective applications in fields of pharmacology and biological medicine (A review of current applications and upcoming potentialities). *Journal of Polymers and the Environment, 29*(8), 2359–2371. https://doi.org/10.1007/s10924-021-02052-2

Mutlu, M., Bingol, Z., Uc, E. M., Köksal, E., Goren, A. C., Alwasel, S. H., & Gulcin, İ. (2023). Comprehensive metabolite profiling of cinnamon (Cinnamomum zeylanicum) leaf oil using LC-HR/MS, GC/MS, and GC-FID: Determination of antiglaucoma, antioxidant, anticholinergic, and antidiabetic profiles. *Life, 13*(1), 136. https://www.mdpi.com/2075-1729/13/1/136.

Niknam, R., Mousavi, M., & Kiani, H. (2020). New studies on the galactomannan extracted from Trigonella foenum-graecum (fenugreek) seed: Effect of subsequent use of ultrasound and microwave on the physicochemical and rheological properties. *Food and Bioprocess Technology, 13*(5), 882–900. https://doi.org/10.1007/s11947-020-02437-6

Noorbakhsh, H., & Khorasgani, M. R. (2023). Functional and chemical properties of Phoenix dactylifera l. Polysaccharides and the effect of date flesh and seed intervention on some blood biomarkers: A contrastive analysis. *Food Chemistry, X, 19,* Article 100834. https://doi.org/10.1016/j.fochx.2023.100834

Shi, H., Wan, Y., Li, O., Zhang, X., Xie, N., Nie, S., & Yin, J. (2020). Two-step hydrolysis method for monosaccharide composition analysis of natural polysaccharides rich in uronic acids. *Food Hydrocolloids, 101,* Article 105524. https://doi.org/10.1016/j.foodhyd.2019.105524

Sorourian, R., Khajehrahimi, A. E., Tadayoni, M., Azizi, M. H., & Hojjati, M. (2022). Structural characterization and cytotoxic, ACE-inhibitory and antioxidant activities of polysaccharide from bitter vetch (Vicia ervilia) seeds. *Journal of Food Measurement and Characterization, 16*(5), 4075–4091. https://doi.org/10.1007/s11694-022-01512-0

Subhash, A. J., Babatunde Bamigbade, G., Al-Ramadi, B., Kamal-Eldin, A., Gan, R.-Y., Senaka Ranadheera, C., & Ayyash, M. (2024). Characterizing date seed polysaccharides: A comprehensive study on extraction, biological activities, prebiotic potential, gut microbiota modulation, and rheology using microwave-assisted deep eutectic solvent. *Food Chemistry, 444,* Article 138618. https://doi.org/10.1016/j.foodchem.2024.138618

Tan, M., Chang, S., Liu, J., Li, H., Xu, P., Wang, P., Wang, X., Zhao, M., Zhao, B., & Wang, L. (2020). Physicochemical properties, antioxidant and antidiabetic activities of polysaccharides from quinoa (Chenopodium quinoa Willd.) seeds. *Molecules, 25* (17), 3840. https://doi.org/10.3390/molecules25173840

Tarique, M., Abdalla, A., Masad, R., Al-Sbiei, A., Kizhakkayil, J., Osaili, T., Olaimat, A., Liu, S.-Q., Fernandez-Cabezudo, M., & Al-Ramadi, B. (2022). Potential probiotics and postbiotic characteristics including immunomodulatory effects of lactic acid bacteria isolated from traditional yogurt-like products. *LWT, 159*, Article 113207. https://doi.org/10.1016/j.lwt.2022.113207

Van den Abbeele, P., Verstrepen, L., Ghyselinck, J., Albers, R., Marzorati, M., & Mercenier, A. (2020). A novel non-digestible, carrot-derived polysaccharide (cRG-I) selectively modulates the human gut microbiota while promoting gut barrier integrity: An integrated in vitro approach. *Nutrients, 12*(7), 1917. https://doi.org/10.3390/nu12071917

Vojvodić Cebin, A., Komes, D., & Ralet, M.-C. (2022). Development and validation of HPLC-DAD method with pre-column PMP derivatization for monomeric profile analysis of polysaccharides from agro-industrial wastes. *Polymers, 14*(3), 544. https://doi.org/10.3390/polym14030544

Wang, Y., Xiong, X., & Huang, G. (2023). Ultrasound-assisted extraction and analysis of maidenhairtree polysaccharides. *Ultrasonics Sonochemistry, 95*, Article 106395. https://doi.org/10.1016/j.ultsonch.2023.106395

Wu, D. T., Feng, K. L., Huang, L., Gan, R. Y., Hu, Y. C., & Zou, L. (2021). Deep eutectic solvent-assisted extraction, partially structural characterization, and bioactivities of acidic polysaccharides from Lotus leaves. *Foods, 10*(10). https://doi.org/10.3390/foods10102330

Yang, J., Zamani, S., Liang, L., & Chen, L. (2021). Extraction methods significantly impact pea protein composition, structure and gelling properties. *Food Hydrocolloids, 117*. https://doi.org/10.1016/j.foodhyd.2021.106678

Yi, C., Xu, L., Luo, C., He, H., Ai, X., & Zhu, H. (2022). In vitro digestion, fecal fermentation, and gut bacteria regulation of brown rice gel prepared from rice slurry backfilled with rice bran. *Food Hydrocolloids, 133*, Article 107986. https://doi.org/10.1016/j.foodhyd.2022.107986

Yılmaz, T., & Şimşek, Ö. (2020). Potential health benefits of ropy exopolysaccharides produced by Lactobacillus plantarum. *Molecules, 25*(14), 3293. https://doi.org/10.3390/molecules25143293

Zeyneb, H., Pei, H., Cao, X., Wang, Y., Win, Y., & Gong, L. (2021). In vitro study of the effect of quinoa and quinoa polysaccharides on human gut microbiota. *Food Science & Nutrition, 9*(10), 5735–5745. https://doi.org/10.1002/fsn3.2540

Zhou, R. R., Huang, J. H., He, D., Yi, Z. Y., Zhao, D., Liu, Z., … Huang, L. Q. (2022). Green and efficient extraction of polysaccharide and ginsenoside from American ginseng (Panax quinquefolius L.) by deep eutectic solvent extraction and aqueous two-phase system. *Molecules, 27*(10). https://doi.org/10.3390/molecules27103132